Chiral Pumping of Spin Waves

Tao Yu,[1] Yaroslav M. Blanter,[1] and Gerrit E. W. Bauer[2,1]
[1] *Kavli Institute of NanoScience, Delft University of Technology, 2628 CJ Delft, Netherlands*
[2] *Institute for Materials Research and WPI-AIMR and CSRN, Tohoku University, Sendai 980-8577, Japan*

(Received 24 August 2019; revised manuscript received 30 October 2019; published 11 December 2019)

We report a theory for the coherent and incoherent chiral pumping of spin waves into thin magnetic films through the dipolar coupling with a local magnetic transducer, such as a nanowire. The ferromagnetic resonance of the nanowire is broadened by the injection of unidirectional spin waves that generates a nonequilibrium magnetization in only half of the film. A temperature gradient between the local magnet and film leads to a unidirectional flow of incoherent magnons, i.e., a chiral spin Seebeck effect.

DOI: 10.1103/PhysRevLett.123.247202

Introduction.—Magnonics and magnon spintronics are fields in which spin waves—the collective excitations of magnetic order—and their quanta, magnons, are studied with the purpose of using them as information carriers in low-power devices [1–4]. Magnons carry angular momentum or "spin" by the precession direction around the equilibrium state. By angular momentum conservation, the magnon spin couples to electromagnetic waves with only one polarization [5], which can be used to control spin waves [1–4]. Surface spin waves or Damon-Eshbach modes also have a handedness or chirality; i.e., their linear momentum is fixed by the outer product of surface normal and magnetization direction [6–9]. Alas, surface magnons have small group velocity, are dephased easily by surface roughness [10], and exist only in sufficiently thick magnetic films, which explains why they have not been employed for applications in magnonic devices [11].

The favored material for magnonics is the ferrimagnetic insulator yttrium iron garnet (YIG) with record low magnetization damping and high Curie temperature [12]. At frequencies up to a few terahertz, YIG is a magnetically soft, simple ferromagnet [13,14]. The long-range dipolar and short-range exchange interactions dominate the spin wave dispersion for long and short wavelengths, respectively, which are of the dipolar, dipolar-exchange, and exchange type over frequencies from a few gigahertz to a few terahertz [1–4]. Long-wavelength dipolar spin waves can be coherently excited by microwaves and travel over centimeters [14], but suffer from low group velocities. Exchange spin waves have much higher group velocity, but they can often be excited only incoherently [15] and are scattered easily with diffuse transport of reduced (micrometer) length scale. The dipolar-exchange spin waves are potentially most suitable for coherent information technologies by combining speed with long lifetime. Recently, short-wavelength dipolar-exchange spin waves have been coherently excited in magnetic films by attaching transducers in the form of thin and narrow ferromagnetic wires or wire arrays with high resonance frequencies [16–22]. Micromagnetic simulations [22] revealed that the ac dipolar field emitted by a cylindrical magnetic wire antenna can excite unidirectional spin waves in a magnetic film with wave vector *parallel* to the magnetization, but no physical arguments or experiments supported this finding. Below we report that the chosen configuration [22] is not optimal and results do not hold for general magnetization directions and realistic nanowires. Recently, nearly perfectly chiral excitation of exchange spin waves was observed in thin YIG films with Co or Ni nanowire gratings with collinear magnetizations [23,24].

The chiral excitation of spin waves [23] corresponds to a robust and switchable exchange magnon current generated by microwaves. The generation of dc currents by ac forces in the absence of a dc bias is referred to as "pumping" [25]. Spin pumping is the injection of a spin current by the magnetization dynamics of a magnet into a contact normal metal by the interface exchange interaction [26,27]. We therefore refer to generation of unidirectional spin waves by the dynamics of a proximity magnetic wire as chiral spin pumping. Here we present a semianalytic theory of chiral pumping of exchange magnons for arbitrary magnetic configurations of the magnetic wire on top of ultrathin (up to tens of nanometers) magnetic films in which the Damon-Eshbach modes do not exist. We distinguish coherent pumping by applied microwaves from the incoherent (thermal) pumping by a temperature difference, i.e., the chiral spin Seebeck effect [28–31], as shown schematically in Fig. 1. The former has been studied by microwave transmission spectroscopy [23,24]. Both effects can be observed via inductive or optical detection schemes. Both processes are caused by the chirality of the dipolar photon-magnon coupling and the physics is very different from that governing the exchange-induced, nonchiral spin pumping and spin Seebeck effect [26–31].

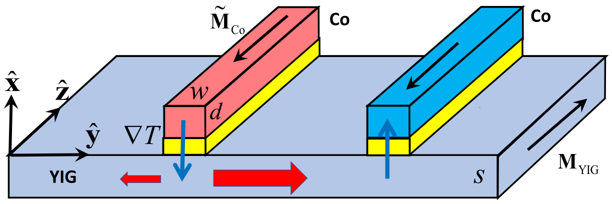

FIG. 1. Chiral spin Seebeck effect. A thin nonmagnetic spacer between the YIG film and Co nanowire (optionally) suppresses the exchange interaction. The magnitude of the magnon currents pumped into the $\pm\hat{\mathbf{y}}$ directions is indicated by the size of the red arrows. Another Co nanowire (the blue one) detects the excited magnons.

Chiral spin pumping turns out to be very anisotropic. When spin waves propagate perpendicular to the magnetization with opposite momenta, their dipolar fields vanish on opposite sides of the film; when propagating parallel to the magnetization, their dipolar field is chiral, i.e., polarization-momentum locked. Purely chiral coupling between magnons can be achieved in the former case without constraints on the degree of polarization of the local magnet. We also find that the pumping by dipolar interaction is chiral in both momentum and real space; i.e., in the configuration of Fig. 1, unidirectional spin waves are excited in half of the film.

Origin of the chiral coupling.—The dynamic dipolar coupling of magnetization $\tilde{\mathbf{M}}$ of the local magnet with that of a film $\mathbf{M}$ by the Zeeman interaction with the respective dipolar magnetic fields $\mathbf{h}$ and $\tilde{\mathbf{h}}$ [32] is

$$\begin{aligned} \hat{H}_{\mathrm{int}}/\mu_0 &= -\int \tilde{\mathbf{M}}(\mathbf{r},t)\cdot\mathbf{h}(\mathbf{r},t)d\mathbf{r} \\ &= -\int \mathbf{M}(\mathbf{r},t)\cdot\tilde{\mathbf{h}}(\mathbf{r},t)d\mathbf{r}, \end{aligned} \tag{1}$$

where μ_0 is the vacuum permeability. We focus here on circularly polarized exchange spin waves in a magnetic film with thickness s at frequency ω and in-plane wave vector $\mathbf{k} = k_y\hat{\mathbf{y}} + k_z\hat{\mathbf{z}}$ in the coordinate system defined in Fig. 1 [the general case is treated in the Supplemental Material (SM), Sec. I. A [33]]. We set out from a classical picture in order to introduce the unique features of the dipolar fields, but use a quantum description to concisely and transparently describe the chiral coupling in terms of Hamiltonian matrix elements. The approximations limit the results to the classical regime, but the formalism can be extended to a future quantum magnonics. The vector field, $M_x(\mathbf{r},t) = m_R^{\mathbf{k}}(x)\cos(\mathbf{k}\cdot\boldsymbol{\rho} - \omega t)$ and $M_y(\mathbf{r},t) \equiv -m_R^{\mathbf{k}}(x)\sin(\mathbf{k}\cdot\boldsymbol{\rho} - \omega t)$, describes the precession around the equilibrium magnetization modulated in the $\hat{\mathbf{z}}$ direction, where $m_R^{\mathbf{k}}(x)$ is the time-independent amplitude normal to the film and $\boldsymbol{\rho} = y\hat{\mathbf{y}} + z\hat{\mathbf{z}}$. The dipolar field outside the film generated by the spin waves,

$$h_\beta(\mathbf{r},t) = \frac{1}{4\pi}\partial_\beta\partial_\alpha\int d\mathbf{r}'\frac{M_\alpha(\mathbf{r}',t)}{|\mathbf{r}-\mathbf{r}'|}, \tag{2}$$

in the summation convention over repeated Cartesian indices $\alpha, \beta = \{x, y, z\}$ [32], becomes

$$\begin{pmatrix} h_x(\mathbf{r},t) \\ h_y(\mathbf{r},t) \\ h_z(\mathbf{r},t) \end{pmatrix} = \begin{pmatrix} (k+\eta k_y)\cos(\mathbf{k}\cdot\boldsymbol{\rho}-\omega t) \\ k_y(k_y/k+\eta)\sin(\mathbf{k}\cdot\boldsymbol{\rho}-\omega t) \\ k_z(k_y/k+\eta)\sin(\mathbf{k}\cdot\boldsymbol{\rho}-\omega t) \end{pmatrix} \times \frac{1}{2}e^{-\eta k x}\int dx' m_R^{\mathbf{k}}(x')e^{\eta k x'}, \tag{3}$$

where the spatial integral is over the film thickness s. $x > 0$ ($x < -s$) is the case with the dipolar field above (below) the film and $\eta = 1$ (-1) when $x > 0$ ($x < -s$), $k = |\mathbf{k}|$. The interaction Hamiltonian Eq. (1) for a wire with thickness d and width w [32] reduces to

$$\hat{H}_{\mathrm{int}}(t) = -\mu_0\int_0^d \hat{\tilde{M}}_\beta(x,\boldsymbol{\rho},t)\hat{h}_\beta(x,\boldsymbol{\rho},t)dx d\boldsymbol{\rho}. \tag{4}$$

The spin waves in the film with $k_z = 0$ propagate normal to the wire with dipolar field $h_z = 0$. The distribution of the dipolar field above and below the film then strongly depends on the wave vector direction: the dipolar field generated by the right (left) moving spin waves vanishes below (above) the film [23] and precesses in the opposite direction of the magnetization, as sketched in Fig. 2. The magnetization in the wire precesses in a direction governed by the magnetization direction and couples only to spin waves with finite dipolar field amplitude in the wire and matched precession [23,24]. We thus understand that the dipolar coupling is chiral and the time-averaged coupling

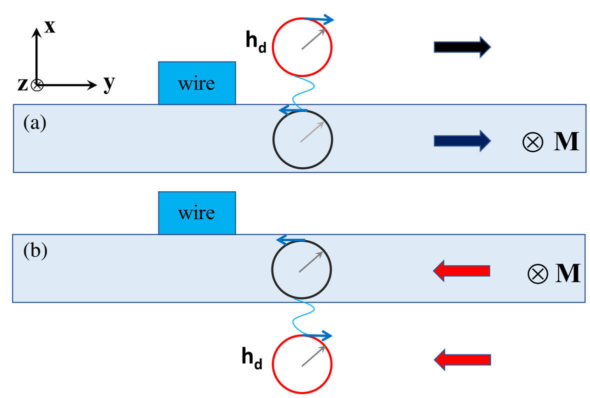

FIG. 2. Half-space dipolar fields generated by spin waves propagating normal to the (equilibrium) magnetization of an in-plane magnetized film ($\mathbf{M}_s \| \hat{\mathbf{z}}$). The fat black arrows in (a) and red arrows in (b) indicate the spin wave propagation direction. The black (red) circles are the precession cones of the film magnetization (corresponding dipolar field) and precession direction is indicated by thin blue arrows.

strength is maximized when the magnetizations of the film and wire are antiparallel.

Spin waves in the film propagating parallel to the magnetization ($k_y = 0 \to h_y = 0$) may also couple chirally to the local magnet, but by a different mechanism. According to Eq. (3), $h_x \propto |k_z| \cos(k_z z - \omega t)$ and $h_z \propto \eta k_z \sin(k_z z - \omega t)$. Above the film, the dipolar fields with positive (negative) k_z are left-circularly (right-circularly) polarized, respectively, while below the film, the polarizations are reversed. These spin waves couple with the magnet on one side of the film only when its transverse magnetization dynamics is right- or left-circularly polarized [22].

A circularly polarized uniform precession in the nanowire always couples chirally with the spin waves in the film (see SM, Secs. I.B and II [33]) for all angles between magnetizations in film and nanowire irrespective of their polarization. When the nanowire Kittel mode is elliptical, the directionality vanishes for one specific angle θ_c. When the nanowire Kittel mode is fully circularly polarized, the coupling strength vanishes and the critical angle $\theta_c = 0$. With $w > d$ and weak magnetic field bias, $\theta_c \simeq \arccos(\sqrt{d/w})$ (see SM, Sec. II [33]), and the chirality can be controlled by weak in-plane magnetic fields.

General formalism.—Here we formulate the general problem of the dynamic dipolar coupling between a nanowire with equilibrium magnetization in contact with an extended thin magnetic film. At resonance, microwaves populate preferentially the collective ("Kittel") modes [37], while a finite temperature populates all magnon modes with a Planck distribution. We focus here on the optimal antiparallel configuration, deferring the derivations and discussions of general situations to the SM, Sec. II [33].

For sufficiently small amplitudes, the Cartesian components $\beta \in \{x, y\}$ of the magnetization dynamics of film ($\hat{\mathbf{M}}$) and nanowire ($\hat{\tilde{\mathbf{M}}}$) can be expanded into magnon creation and annihilation operators [10,38,39],

$$\hat{M}_\beta(\mathbf{r}) = -\sqrt{2M_s\gamma\hbar}\sum_{\mathbf{k}}[m_\beta^{(\mathbf{k})}(x)e^{i\mathbf{k}\cdot\boldsymbol{\rho}}\hat{\alpha}_{\mathbf{k}} + \text{H.c.}],$$

$$\hat{\tilde{M}}_\beta(\mathbf{r}) = -\sqrt{2\tilde{M}_s\gamma\hbar}\sum_{k_z}[\tilde{m}_\beta^{(k_z)}(x,y)e^{ik_z z}\hat{\beta}_{k_z} + \text{H.c.}], \quad (5)$$

where M_s and $\tilde{M}_s$ are the saturation magnetizations, $-\gamma$ is the gyromagnetic ratio, $m_\beta^{(\mathbf{k})}(x)$ and $\tilde{m}_\beta^{(k_z)}(x,y)$ are the spin wave amplitudes across the film and nanowire, and $\hat{\alpha}_{\mathbf{k}}$ and $\hat{\beta}_{k_z}$ denote the magnon (annihilation) operator in the film and nanowire, respectively.

We are mainly interested in high-quality ultrathin films and nanowires with $s, d \gtrsim \mathcal{O}(10\text{ nm})$ and nanowire width $w \gtrsim \mathcal{O}(50\text{ nm})$, such that the magnetization across the film and nanowire (centered at $y_0\hat{\mathbf{y}}$) is nearly homogeneous: $m_\beta^{(\mathbf{k})}(x) \approx m_\beta^{(\mathbf{k})}\Theta(-x)\Theta(x+s)$ and $\tilde{m}_\beta^{(k_z)}(x,y) \approx \tilde{m}_\beta^{(k_z)}\Theta(x)\Theta(-x+d)\Theta(y-y_0+w/2)\Theta(-y+y_0+w/2)$, with $\Theta(x)$ the Heaviside step function [21,23,24]. We consider here only pure exchange magnons since the dipolar intrafilm interactions are negligibly small for sufficiently thin films and/or high frequencies. Disregarding higher magnon subbands turns out to be a good approximation even at higher temperatures because of the strong mode selectivity of the dipolar coupling [33]. Here we disregard interface exchange, which appears to play only a minor role [23,24]. The system Hamiltonian then becomes

$$\hat{H}/\hbar = \sum_{\mathbf{k}}\omega_{\mathbf{k}}\hat{\alpha}_{\mathbf{k}}^\dagger\hat{\alpha}_{\mathbf{k}} + \sum_{k_z}\tilde{\omega}_{k_z}\hat{\beta}_{k_z}^\dagger\hat{\beta}_{k_z} + \sum_{\mathbf{k}}(g_{\mathbf{k}}e^{-ik_y y_0}\hat{\alpha}_{\mathbf{k}}^\dagger\hat{\beta}_{k_z} + g_{\mathbf{k}}^* e^{ik_y y_0}\hat{\beta}_{k_z}^\dagger\hat{\alpha}_{\mathbf{k}}), \quad (6)$$

where $\omega_{\mathbf{k}}$ and $\tilde{\omega}_{k_z}$ are the frequencies of spin waves in the film and nanowire and, with Eqs. (2), (4), and (5), the coupling

$$g_{\mathbf{k}} = F(\mathbf{k})(m_x^{(\mathbf{k})*}, m_y^{(\mathbf{k})*})\begin{pmatrix} |\mathbf{k}| & ik_y \\ ik_y & -k_y^2/|\mathbf{k}| \end{pmatrix}\begin{pmatrix} \tilde{m}_x^{(k_z)} \\ \tilde{m}_y^{(k_z)} \end{pmatrix}, \quad (7)$$

with $F(\mathbf{k}) = -\mu_0\gamma\sqrt{M_s\tilde{M}_s/L}\phi(\mathbf{k})$. The form factor $\phi(\mathbf{k}) = 2\sin(k_y w/2)(1-e^{-kd})(1-e^{-ks})/(k_y k^2)$ couples spin waves with wavelengths of the order of the nanowire width (mode selection) and $\lim_{\mathbf{k}\to 0}\phi(\mathbf{k}) = wsd$. Exchange waves are right-circularly polarized with $m_y^{(k_y)} = im_x^{(k_y)}$ and the coupling is perfectly chiral $g_{-|k_y|} = 0$.

The linear response to microwave and thermal excitations can be described by the input-output theory [40,41] and by a Kubo formula (see SM, Sec. III [33]). Let $\hat{p}_{k_z}(t) = \int \hat{p}_{k_z}(\omega)e^{-i\omega t}d\omega/(2\pi)$ be a microwave photon input centered at the frequency $\tilde{\omega}_{k_z}$: $\langle\hat{p}_{k_z}(\omega)\rangle \to 2\pi\mathcal{D}\delta(\omega - \tilde{\omega}_{k_z})$ with amplitude $\mathcal{D}$, the equations of motion are [40,41]

$$\frac{d\hat{\beta}_{k_z}}{dt} = -i\tilde{\omega}_{k_z}\hat{\beta}_{k_z}(t) - \sum_{k_y} ig_{\mathbf{k}}^* e^{ik_y y_0}\hat{\alpha}_{\mathbf{k}}(t) - \left(\frac{\tilde{\kappa}_{k_z}}{2} + \frac{\zeta_{k_z}}{2}\right)\hat{\beta}_{k_z}(t) - \sqrt{\tilde{\kappa}_{k_z}}\hat{\tilde{N}}_{k_z}(t) - \sqrt{\zeta_{k_z}}\hat{p}_{k_z}(t),$$

$$\frac{d\hat{\alpha}_{\mathbf{k}}}{dt} = -i\omega_{\mathbf{k}}\hat{\alpha}_{\mathbf{k}}(t) - ig_{\mathbf{k}}e^{-ik_y y_0}\hat{\beta}_{k_z}(t) - \frac{\kappa_{\mathbf{k}}}{2}\hat{\alpha}_{\mathbf{k}}(t) - \sqrt{\kappa_{\mathbf{k}}}\hat{N}_{\mathbf{k}}(t), \quad (8)$$

where $\tilde{\kappa}_{k_z} \equiv 2\tilde{\chi}\tilde{\omega}_{k_z}$ ($\kappa_{\mathbf{k}} \equiv 2\chi\omega_{\mathbf{k}}$) is the damping rates in terms of the Gilbert damping constant $\tilde{\chi}(\chi)$ in the nanowire (film) and ζ_{k_z} is the radiative damping. The thermal environment of the magnetic film causes fluctuations $\hat{N}_{\mathbf{k}}$ [41] generated by a Markovian process that obeys the (quantum) fluctuation-dissipation theorem with $\langle\hat{N}_{\mathbf{k}}\rangle = 0$ and $\langle\hat{N}_{\mathbf{k}}^\dagger(t)\hat{N}_{\mathbf{k}'}(t')\rangle = n_{\mathbf{k}}\delta(t-t')\delta_{\mathbf{k}\mathbf{k}'}$. $n_{\mathbf{k}} = 1/\{\exp[\hbar\omega_{\mathbf{k}}/(k_B T_2)] - 1\}$ is the magnon population at temperature T_2 of film, and $k_B T_2$ should be larger than $\hbar\omega_{\mathbf{k}}$. The thermal fluctuations $\hat{\tilde{N}}_{k_z}$ in the nanowire are characterized by a different temperature T_1 and thermal magnon distribution, $\tilde{n}_{k_z} = 1/\{\exp[\hbar\tilde{\omega}_{k_z}/(k_B T_1)] - 1\}$. The solutions

$$\hat{\beta}_{k_z}(\omega) = \frac{i\sum_{k_y}\gamma_{\mathbf{k}}G_{\mathbf{k}}\hat{N}_{\mathbf{k}}(\omega) - \sqrt{\tilde{\kappa}_{k_z}}\hat{\tilde{N}}_{k_z}(\omega) - \sqrt{\zeta_{k_z}}\hat{p}_{k_z}(\omega)}{-i(\omega - \tilde{\omega}_{k_z}) + \frac{\tilde{\kappa}_{k_z}}{2} + \frac{\zeta_{k_z}}{2} + i\sum_{k_y}|g_{\mathbf{k}}|^2 G_{\mathbf{k}}(\omega)},$$

$$\hat{\alpha}_{\mathbf{k}}(\omega) = G_{\mathbf{k}}(\omega)[g_{\mathbf{k}}e^{-ik_y y_0}\hat{\beta}_{k_z}(\omega) - i\sqrt{\kappa_{\mathbf{k}}}\hat{N}_{\mathbf{k}}(\omega)], \tag{9}$$

with the Green function $G_{\mathbf{k}}(\omega) = [(\omega - \omega_{\mathbf{k}}) + i\kappa_{\mathbf{k}}/2]^{-1}$ and $\gamma_{\mathbf{k}} = ig^*_{\mathbf{k}}e^{ik_y y_0}\sqrt{\kappa_{\mathbf{k}}}$, reveal that the thermal fluctuations in both wire ($\hat{\tilde{N}}_{k_z}$) and film ($\hat{N}_{\mathbf{k}}$) affect $\hat{\beta}_{k_z}(\omega)$. Moreover, the interaction enhances the damping of nanowire spin waves by $\delta\tilde{\kappa}_{k_z} = 2\pi\sum_{k_y}|g_{\mathbf{k}}|^2\delta(\tilde{\omega}_{k_z} - \omega_{\mathbf{k}})$ to $\tilde{\kappa}'_{k_z}$ and shifts the frequency to $\tilde{\omega}'_{k_z}$. Chiral pumping can be realized by coherent microwave excitation or the incoherent excitation by a temperature difference between the local magnet and film, as shown in the following.

Coherent chiral pumping.—A uniform microwave field excites only the Kittel mode ($k_z = 0$) in the nanowire. Spin waves in the film with finite $k_y \equiv q$ are excited indirectly by the inhomogeneous stray field of the wire. The coherent chiral pumping by microwaves at thermal equilibrium with $T_1 = T_2 \equiv T_0$ reads

$$\hat{\alpha}_q(t) = \int\frac{d\omega}{2\pi}\frac{e^{-i\omega t}ig_q e^{-iqy_0}}{-i(\omega - \omega_q) + \frac{\kappa_q}{2}}\frac{\sqrt{\zeta_0}\hat{p}_0(\omega)}{-i(\omega - \tilde{\omega}'_0) + \frac{\tilde{\kappa}'_0}{2} + \frac{\zeta_0}{2}}. \tag{10}$$

Since the magnons are coherently excited, their number is $\langle\hat{\alpha}^\dagger_q(t)\hat{\alpha}_q(t)\rangle = \langle\hat{\alpha}^\dagger_q(t)\rangle\langle\hat{\alpha}_q(t)\rangle$. In the absence of damping, κ_q is a positive infinitesimal that safeguards causality. A resonant input $\langle\hat{p}_0\rangle = 2\pi\mathcal{D}\delta(\omega - \tilde{\omega}_0)$ excites a film magnetization in position space,

$$\delta M_\beta(\mathbf{r}) = \sqrt{2M_s\gamma\hbar}\mathcal{D}\frac{1}{v_{q_*}}\frac{e^{-i\tilde{\omega}_0 t}\sqrt{\zeta_0}}{(\tilde{\omega}_0 - \tilde{\omega}'_0) + i(\tilde{\kappa}'_0 + \zeta_0)/2} \times \begin{cases} m_\beta^{(q_*)}(x)g_{q_*}e^{iq_+(y-y_0)} + \text{H.c.} & y > y_0 \\ m_\beta^{(-q_*)}(x)g_{-q_*}e^{iq_-(y-y_0)} + \text{H.c.} & y < y_0, \end{cases} \tag{11}$$

where $\tilde{\omega}_0 - \omega_q + i\kappa_q/2$ vanishes for $q_\pm = \pm(q_* + i\delta_\Gamma)$ with $q_* > 0$ and inverse propagation length δ_Γ, and $v_{q_*} = \partial\omega_q/\partial q|_{q_*}$ is the magnon group velocity. For perfect chiral coupling, $g_{-q_*} = 0$, only the magnetization in half-space $y > y_0$ can be excited, which implies handedness also in position space.

The coherent chiral pumping can be directly observed by microwave transmission spectra [17,20,21]. We here let two nanowires at $\mathbf{r}_1 = R_1\hat{\mathbf{y}}$ and $\mathbf{r}_2 = R_2\hat{\mathbf{y}}$ act as excitation and detection transducers. The spin wave transmission amplitude as derived and calculated in the SM, Sec. IV [33], reads

$$S_{21}(\omega) = \frac{[1 - S_{11}(\omega)]\sum_q iG_q(\omega)|g_q|^2 e^{iq(R_2 - R_1)}}{-i(\omega - \tilde{\omega}_0) + \tilde{\kappa}_0/2 + i\sum_q G_q(\omega)|g_q|^2}, \tag{12}$$

and the reflection amplitude $S_{11}(\omega)$ is given in the SM. Chirality enters via the phase factor $e^{iq(R_2 - R_1)}$: When $g_{-|q|} = 0$, spin and microwaves are transmitted from 1 to 2 only when $R_2 > R_1$.

Incoherent chiral pumping.—Spin waves can be incoherently excited by locally heating the nanowire, e.g., by the Joule heating due to an applied current [15]. In the absence of microwaves, $\hat{p}_{k_z} = 0$, the magnon distribution of the film reads

$$f(\mathbf{k}) \equiv \langle\hat{\alpha}^\dagger_{\mathbf{k}}(t)\hat{\alpha}_{\mathbf{k}}(t)\rangle = n_{\mathbf{k}} + \frac{|g_{\mathbf{k}}|^2}{(\omega_{\mathbf{k}} - \tilde{\omega}'_{k_z})^2 + (\tilde{\kappa}'_{k_z}/2)^2}\frac{\tilde{\kappa}_{k_z}}{\kappa_{\mathbf{k}}}(\tilde{n}_{k_z} - n_{\mathbf{k}}). \tag{13}$$

When $T_1 > T_2$, magnons are injected from the local magnet into the film. When the coupling is chiral with $g_{\mathbf{k}} \neq g_{-\mathbf{k}}$, the distribution of magnons is asymmetric, $f(\mathbf{k}) \neq f(-\mathbf{k})$, i.e., carries a unidirectional spin current $I \propto \sum_{\mathbf{k}} v_{\mathbf{k}} f(\mathbf{k})$, which in turn generates a magnon accumulation in the detector magnet.

All occupied modes in the local magnet contribute to the excitation of the film. The excited magnon density for $y > y_0$ in a high-quality film with $\kappa_{\mathbf{k}} \to 0_+$ reads

$$\delta\rho_> \equiv \langle\hat{\alpha}^\dagger(\boldsymbol{\rho}, t)\hat{\alpha}(\boldsymbol{\rho}, t)\rangle|_{y>y_0} - \sum_{\mathbf{k}} n_{\mathbf{k}} = \sum_{k_z}\int\frac{d\omega}{2\pi}(\tilde{n}_{k_z} - n_{\mathbf{k}_\omega})\frac{|g_{\mathbf{k}_\omega}|^2}{v^2_{\mathbf{k}_\omega}}\frac{\tilde{\kappa}_{k_z}}{(\omega - \tilde{\omega}'_{k_z})^2 + (\tilde{\kappa}'_{k_z}/2)^2}, \tag{14}$$

where $\mathbf{k}_\omega = q_\omega\hat{\mathbf{y}} + k_z\hat{\mathbf{z}}$ and q_ω is the positive root of $\omega_{q_\omega,k_z} = \omega$. For weak magnetic damping in the wire $\tilde{\kappa}_m \ll \tilde{\omega}_m$, the rhs reduces to $\delta\rho_> \approx \sum_{k_z}(|g_{q_*,k_z}|^2/v^2_{q_*,k_z})\times(\tilde{n}_{k_z} - n_{q_*,k_z})$ and $\omega_{q_*,k_z} = \tilde{\omega}_{k_z}$. For $y < y_0$, $\delta\rho_< \approx \sum_{k_z}(|g_{-q_*,k_z}|^2/v^2_{q_*,k_z})(\tilde{n}_{k_z} - n_{q_*,k_z}) \neq \delta\rho_>$. We conclude that the thermal injection via chiral coupling leads to different magnon densities on both sides of the nanowire. This is a chiral equivalent of the conventional spin Seebeck effect [28–31].

The chiral pumping of magnons can be detected inductively via microwave emission of a second magnetic wire, by Brillouin light scattering [24,42], NV center magnetometry [43], and electrically by the inverse spin Hall effect [15]. The incoherent excitation couples strongly only with the long-wavelength modes that propagate ballistically over large distances, and the effect is most efficiently detected by a mode-selective spectroscopy. The thermally excited population of the Kittel mode in the (right) detection transducer reads (see derivation and discussion in SM, Sec. V [33])

$$\delta\rho_R = \int \frac{d\omega}{2\pi} \frac{\Gamma_1^2 \tilde{\kappa}_0 (n_L - n_{q_*})}{[(\omega - \omega_K)^2 + (\tilde{\kappa}_0/2 + \Gamma_1/2)^2]^2}, \tag{15}$$

where ω_K is the Kittel mode frequency of the nanowires, $n_L = 1/\{\exp[\hbar\omega_K/(k_B T_2)] - 1\}$ and $n_{q_*} = 1/\{\exp[\hbar\omega_K/(k_B T_1)] - 1\}$ are magnon numbers in left and right wires, respectively, and $\Gamma_1 = |g_{q_*}|^2/v_{q_*}$ is the dissipative coupling mediated by the magnons in the film. The reference's signal is given by the parallel magnetization configuration of wires and film since $g_{q_*} = 0$ and the right transducer is not affected.

Finally, we present numerical estimates for the observables. The dipolar pumping causes additional damping $\delta\chi = \delta\tilde{\kappa}_0/(2\tilde{\omega}_0)$ and broadening of the ferromagnetic resonance spectrum of the nanowire. In a detector wire at a distance, the thermally pumped magnon density $\delta\rho_>$ in the film injects Kittel mode magnons $\delta\rho_R$. We consider a Co nanowire with width $w = 70$ nm and thickness $d = 20$ nm. The magnetization $\mu_0 \tilde{M}_s = 1.1$ T [21,24], the exchange stiffness $\tilde{\lambda}_{\mathrm{ex}} = 3.1 \times 10^{-13}$ cm^2 [44], and the Gilbert damping coefficient $\alpha_{\mathrm{Co}} = 2.4 \times 10^{-3}$ [45]. For the YIG film $s = 20$ nm with magnetization $\mu_0 M_s = 0.177$ T and exchange stiffness $\lambda_{\mathrm{ex}} = 3.0 \times 10^{-12}$ cm^2 [10,21,24]. A magnetic field $\mu_0 H_{\mathrm{app}} = 0.05$ T is sufficient to switch the film magnetizations antiparallel to that of the wire [20,21]. The calculated additional damping of nanowire Kittel dynamics is then $\delta\chi_{\mathrm{Co}} = 3.1 \times 10^{-2}$, which is one order of magnitude larger than the intrinsic one. The chiral spin Seebeck effect is most easily resolved at low temperatures. With $T_2 = 30$ K and $T_1 = 10$ K, $\delta\rho_> = 4 \times 10^{13}$ cm^{-2}, $\delta\rho_< = 2 \times 10^{13}$ cm^{-2}, on top of the thermal equilibrium $\sum_{\mathbf{k}} n_{\mathbf{k}} = 3 \times 10^{12}$ cm^{-2}. The number of thermally injected Kittel magnons in the detector $\delta\rho_R \approx 10$ should be compared to the background one $n_{q_*} \approx 38$. The numbers can be strongly increased by choosing narrower nanowires with a better chirality and placing more than one nanowire within the spin wave propagation length, since the signals should approximately add up. The population of tens of magnons [23,24] should be well within the signal-to-noise ratio of Brillouin light scattering [46,47], but more difficult to be detected electrically [48].

Discussion.—In conclusion, we developed a general theory of directional (chiral) pumping of exchange spin waves in ultrathin magnetic films. The dipolar coupling is a relatively long-range interaction between two magnetic bodies, which at intermagnetic interfaces competes with the strong, but very short-range exchange interaction that can easily be suppressed by inserting a nonmagnetic spacer layer [18,19,21,24]. We illustrate the general theory for Co nanowires on YIG films [21,23,24]. Other material combinations can be treated in principle as well by changing the model parameters. Chirality is most efficiently generated when the magnetizations are antiparallel. Partial chiral spin pumping persists when the magnetizations of the film and nanowire are perpendicular [22], but then it depends on the geometry and the coupling strength is reduced. Our study is closely related to the field of chiral optics [5] that focuses on electric dipoles. The chirality of the magnetic dipolar field can be considered as the low-frequency limit of chiral optics and plasmonics, in which retardation can be disregarded [5,49,50]. We envision cross-fertilization between optical metamaterials and magnonics, stimulating activities such as nanorouting of magnons [49,50].

This work is financially supported by the Nederlandse Organisatie voor Wetenschappelijk Onderzoek (NWO) as well as JSPS KAKENHI Grant No. 26103006. We thank Professor Haiming Yu for useful discussions.

[1] B. Lenk, H. Ulrichs, F. Garbs, and M. Münzenberg, Phys. Rep. **507**, 107 (2011).
[2] A. V. Chumak, V. I. Vasyuchka, A. A. Serga, and B. Hillebrands, Nat. Phys. **11**, 453 (2015).
[3] D. Grundler, Nat. Nanotechnol. **11**, 407 (2016).
[4] V. E. Demidov, S. Urazhdin, G. de Loubens, O. Klein, V. Cros, A. Anane, and S. O. Demokritov, Phys. Rep. **673**, 1 (2017).
[5] P. Lodahl, S. Mahmoodian, S. Stobbe, A. Rauschenbeutel, P. Schneeweiss, J. Volz, H. Pichler, and P. Zoller, Nature (London) **541**, 473 (2017).
[6] L. R. Walker, Phys. Rev. **105**, 390 (1957).
[7] R. W. Damon and J. R. Eshbach, J. Phys. Chem. Solids **19**, 308 (1961).
[8] A. Akhiezer, V. Baríakhtar, and S. Peletminski, *Spin Waves* (North-Holland, Amsterdam, 1968).
[9] D. D. Stancil and A. Prabhakar, *Spin Waves—Theory and Applications* (Springer, New York, 2009).
[10] T. Yu, S. Sharma, Y. M. Blanter, and G. E. W. Bauer, Phys. Rev. B **99**, 174402 (2019).
[11] M. Jamali, J. H. Kwon, S.-M. Seo, K.-J. Lee, and H. Yang, Sci. Rep. **3**, 3160 (2013).
[12] H. Chang, P. Li, W. Zhang, T. Liu, A. Hoffmann, L. Deng, and M. Wu, IEEE Magn. Lett. **5**, 1 (2014).
[13] V. Cherepanov, I. Kolokolov, and V. L'vov, Phys. Rep. **229**, 81 (1993).
[14] A. A. Serga, A. V. Chumak, and B. Hillebrands, J. Phys. D **43**, 264002 (2010).
[15] L. J. Cornelissen, J. Liu, R. A. Duine, J. B. Youssef, and B. J. van Wees, Nat. Phys. **11**, 1022 (2015).
[16] *Nanomagnetism and Spintronics*, edited by T. Shinjo (Elsevier, Oxford, 2009).
[17] H. Yu, G. Duerr, R. Huber, M. Bahr, T. Schwarze, F. Brandl, and D. Grundler, Nat. Commun. **4**, 2702 (2013).
[18] H. Qin, S. J. Hämäläinen, and S. van Dijken, Sci. Rep. **8**, 5755 (2018).

[19] S. Klingler, V. Amin, S. Geprägs, K. Ganzhorn, H. Maier-Flaig, M. Althammer, H. Huebl, R. Gross, R. D. McMichael, M. D. Stiles, S. T. B. Goennenwein, and M. Weiler, Phys. Rev. Lett. **120**, 127201 (2018).
[20] C. P. Liu *et al.*, Nat. Commun. **9**, 738 (2018).
[21] J. L. Chen, C. P. Liu, T. Liu, Y. Xiao, K. Xia, G. E. W. Bauer, M. Z. Wu, and H. M. Yu, Phys. Rev. Lett. **120**, 217202 (2018).
[22] Y. Au, E. Ahmad, O. Dmytriiev, M. Dvornik, T. Davison, and V. V. Kruglyak, Appl. Phys. Lett. **100**, 182404 (2012).
[23] T. Yu, C. P. Liu, H. M. Yu, Y. M. Blanter, and G. E. W. Bauer, Phys. Rev. B **99**, 134424 (2019).
[24] J. L. Chen, T. Yu, C. P. Liu, T. Liu, M. Madami, K. Shen, J. Y. Zhang, S. Tu, M. S. Alam, K. Xia, M. Z. Wu, G. Gubbiotti, Y. M. Blanter, G. E. W. Bauer, and H. M. Yu, Phys. Rev. B **100**, 104427 (2019).
[25] M. Büttiker, H. Thomas, and A. Prêtre, Z. Phys. B **94**, 133 (1994).
[26] Y. Tserkovnyak, A. Brataas, and G. E. W. Bauer, Phys. Rev. Lett. **88**, 117601 (2002).
[27] Y. Tserkovnyak, A. Brataas, G. E. W. Bauer, and B. I. Halperin, Rev. Mod. Phys. **77**, 1375 (2005).
[28] K. Uchida, J. Xiao, H. Adachi, J. Ohe, S. Takahashi, J. Ieda, T. Ota, Y. Kajiwara, H. Umezawa, H. Kawai, G. E. W. Bauer, S. Maekawa, and E. Saitoh, Nat. Mater. **9**, 894 (2010).
[29] J. Xiao, G. E. W. Bauer, K. C. Uchida, E. Saitoh, and S. Maekawa, Phys. Rev. B **81**, 214418 (2010).
[30] H. Adachi, J. I. Ohe, S. Takahashi, and S. Maekawa, Phys. Rev. B **83**, 094410 (2011).
[31] G. E. W. Bauer, E. Saitoh, and B. J. van Wees, Nat. Mater. **11**, 391 (2012).
[32] L. D. Landau and E. M. Lifshitz, *Electrodynamics of Continuous Media*, 2nd ed. (Butterworth-Heinenann, Oxford, 1984).
[33] See Supplemental Material at http://link.aps.org/supplemental/10.1103/PhysRevLett.123.247202 for derivations of the dipolar field and interlayer dipolar coupling, the magnetization excitation by linear response, the scattering matrix and dipolar Seebeck effect, which includes Refs [15,34–36].
[34] L. Novotny and B. Hecht, *Principles of Nano-Optics* (Cambridge University Press, Cambridge, England, 2006).
[35] G. D. Mahan, *Many Particle Physics* (Plenum, New York, 1990).
[36] E. Šimánek and B. Heinrich, Phys. Rev. B **67**, 144418 (2003).
[37] C. Kittel, Phys. Rev. **73**, 155 (1948).
[38] C. Kittel, *Quantum Theory of Solids* (Wiley, New York, 1963).
[39] T. Holstein and H. Primakoff, Phys. Rev. **58**, 1098 (1940).
[40] C. W. Gardiner and M. J. Collett, Phys. Rev. A **31**, 3761 (1985).
[41] A. A. Clerk, M. H. Devoret, S. M. Girvin, F. Marquardt, and R. J. Schoelkopf, Rev. Mod. Phys. **82**, 1155 (2010).
[42] S. O. Demokritov, B. Hillebrands, and A. N. Slavin, Phys. Rep. **348**, 441 (2001).
[43] T. van der Sar, F. Casola, R. L. Walsworth, and A. Yacoby, Nat. Commun. **6**, 7886 (2015).
[44] R. Moreno, R. F. L. Evans, S. Khmelevskyi, M. C. Muñoz, R. W. Chantrell, and O. Chubykalo-Fesenko, Phys. Rev. B **94**, 104433 (2016).
[45] M. A. W. Schoen, D. Thonig, M. L. Schneider, T. J. Silva, H. T. Nembach, O. Eriksson, O. Karis, and J. M. Shaw, Nat. Phys. **12**, 839 (2016).
[46] A. Ercole, W. S. Lew, G. Lauhoff, E. T. M. Kernohan, J. Lee, and J. A. C. Bland, Phys. Rev. B **62**, 6429 (2000).
[47] T. Sebastian, K. Schultheiss, B. Obry, B. Hillebrands, and H. Schultheiss, Front. Phys. **3**, 35 (2015).
[48] L. J. Cornelissen, K. J. H. Peters, G. E. W. Bauer, R. A. Duine, and B. J. van Wees, Phys. Rev. B **94**, 014412 (2016).
[49] F. J. Rodríguez-Fortuño, G. Marino, P. Ginzburg, D. O'Connor, A. Martínez, G. A. Wurtz, and A. V. Zayats, Science **340**, 328 (2013).
[50] J. Petersen, J. Volz, and A. Rauschenbeutel, Science **346**, 67 (2014).

Chiral Pumping of Spin Waves: Supplemental Material

Tao Yu and Yaroslav M. Blanter

Kavli Institute of NanoScience, Delft University of Technology, 2628 CJ Delft, The Netherlands

Gerrit E. W. Bauer

Institute for Materials Research & WPI-AIMR & CSRN,
Tohoku University, Sendai 980-8577, Japan and
Kavli Institute of NanoScience, Delft University of Technology, 2628 CJ Delft, The Netherlands

(Dated: August 24, 2019)

I. MAGNETO-DIPOLAR FIELDS

A. In-plane magnetized films

Here we derive the dipolar field generated by spin waves in a magnetic film with arbitrary propagation direction and ellipticity of the polarization. The equilibrium magnetization of the film is along the $\hat{\mathbf{z}}$-direction. The transverse magnetization fluctuations are in general elliptical, i.e., a superposition of the right (m_R) and left (m_L) circular polarized components,

$$\begin{pmatrix} M_x(\mathbf{r}) \\ M_y(\mathbf{r}) \end{pmatrix} = \begin{pmatrix} m_x^{\mathbf{k}}(x)\cos(\mathbf{k}\cdot\boldsymbol{\rho}-\omega t) \\ -m_y^{\mathbf{k}}(x)\sin(\mathbf{k}\cdot\boldsymbol{\rho}-\omega t) \end{pmatrix} = m_R^{\mathbf{k}}(x)\begin{pmatrix} \cos(\mathbf{k}\cdot\boldsymbol{\rho}-\omega t) \\ -\sin(\mathbf{k}\cdot\boldsymbol{\rho}-\omega t) \end{pmatrix} + m_L^{\mathbf{k}}(x)\begin{pmatrix} \cos(\mathbf{k}\cdot\boldsymbol{\rho}-\omega t) \\ \sin(\mathbf{k}\cdot\boldsymbol{\rho}-\omega t) \end{pmatrix},$$

where $m_R^{\mathbf{k}}(x) = [m_x^{\mathbf{k}}(x) + m_y^{\mathbf{k}}(x)]/2$ and $m_L^{\mathbf{k}}(x) = [m_x^{\mathbf{k}}(x) - m_y^{\mathbf{k}}(x)]/2$. This magnetization generates the dipolar field ($\alpha, \beta \in \{x, y, z\}$)

$$h_\beta(\mathbf{r}) = \frac{1}{4\pi}\partial_\beta\partial_\alpha \int d\mathbf{r}' \frac{M_\alpha(\mathbf{r}')}{|\mathbf{r}-\mathbf{r}'|}. \tag{1}$$

Outside the film

$$\begin{aligned}\begin{pmatrix} h_x(\mathbf{r}) \\ h_y(\mathbf{r}) \\ h_z(\mathbf{r}) \end{pmatrix} &= \frac{1}{2}\begin{pmatrix} (|\mathbf{k}| + \mathrm{sgn}(x)k_y)\cos(\mathbf{k}\cdot\boldsymbol{\rho}-\omega t) \\ k_y\left(\frac{k_y}{|\mathbf{k}|} + \mathrm{sgn}(x)\right)\sin(\mathbf{k}\cdot\boldsymbol{\rho}-\omega t) \\ k_z\left(\frac{k_y}{|\mathbf{k}|} + \mathrm{sgn}(x)\right)\sin(\mathbf{k}\cdot\boldsymbol{\rho}-\omega t) \end{pmatrix} e^{-|\mathbf{k}||x|}\int dx' m_R^{\mathbf{k}}(x')\, e^{|\mathbf{k}|\mathrm{sgn}(x)x'} \\ &+ \frac{1}{2}\begin{pmatrix} (|\mathbf{k}| - \mathrm{sgn}(x)k_y)\cos(\mathbf{k}\cdot\boldsymbol{\rho}-\omega t) \\ k_y\left(-\frac{k_y}{|\mathbf{k}|} + \mathrm{sgn}(x)\right)\sin(\mathbf{k}\cdot\boldsymbol{\rho}-\omega t) \\ k_z\left(-\frac{k_y}{|\mathbf{k}|} + \mathrm{sgn}(x)\right)\sin(\mathbf{k}\cdot\boldsymbol{\rho}-\omega t) \end{pmatrix} e^{-|\mathbf{k}||x|}\int dx' m_L^{\mathbf{k}}(x')\, e^{|\mathbf{k}|\mathrm{sgn}(x)x'},\end{aligned} \tag{2}$$

where $\mathrm{sgn}(x)$ is the sign function.

The dipolar field above the film generated by a spin wave propagating normal to the magnetization ($k_z \to 0$) reads [1]

$$\begin{aligned}\begin{pmatrix} h_x(\mathbf{r}) \\ h_y(\mathbf{r}) \end{pmatrix} &= \frac{|k_y| + k_y}{2}\begin{pmatrix} \cos(k_y y-\omega t) \\ \sin(k_y y-\omega t) \end{pmatrix} e^{-|k_y|x}\int dx' m_R^{k_y}(x')\, e^{|k_y|x'} \\ &+ \frac{|k_y| - k_y}{2}\begin{pmatrix} \cos(k_y y-\omega t) \\ -\sin(k_y y-\omega t) \end{pmatrix} e^{-|k_y|x}\int dx' m_L^{k_y}(x')\, e^{|k_y|x'},\end{aligned} \tag{3}$$

while below the film

$$\begin{aligned}\begin{pmatrix} h_x(\mathbf{r}) \\ h_y(\mathbf{r}) \end{pmatrix} &= \frac{|k_y| - k_y}{2}\begin{pmatrix} \cos(k_y y-\omega t) \\ \sin(k_y y-\omega t) \end{pmatrix} e^{|k_y|x}\int dx' m_R^{k_y}(x')\, e^{-|k_y|x'} \\ &+ \frac{|k_y| + k_y}{2}\begin{pmatrix} \cos(k_y y-\omega t) \\ -\sin(k_y y-\omega t) \end{pmatrix} e^{|k_y|x}\int dx' m_L^{k_y}(x')\, e^{-|k_y|x'}.\end{aligned} \tag{4}$$

Spin waves with right circular polarization generate a dipolar field with left circular polarization. Right (left) propagating spin waves with $k_y > 0$ ($k_y < 0$) only generate dipolar field above (below) the film. Spin waves propagating parallel to the equilibrium magnetization ($k_y \to 0$) generate the fields

$$\begin{pmatrix} h_x(\mathbf{r}) \\ h_z(\mathbf{r}) \end{pmatrix} = \frac{1}{2}\begin{pmatrix} |k_z|\cos(\mathbf{k}\cdot\boldsymbol{\rho}-\omega t) \\ \mathrm{sgn}\,(x)\,k_z\sin(\mathbf{k}\cdot\boldsymbol{\rho}-\omega t) \end{pmatrix} e^{-|k_z||x|}\int dx'\left(m_R^{k_z}(x')+m_L^{k_z}(x')\right)e^{|k_z|\mathrm{sgn}(x)x'}.$$

Above the film, the dipolar field of spin waves with positive (negative) k_z, is always left (right) circularly polarized, viz. polarization-momentum locked. Below the film, the polarization is reversed.

B. Magnetic nanowire

Here we consider the dipolar field generated by a circularly polarized Kittel mode and show that its Fourier components are chiral. We consider a nanowire and its equilibrium magnetization along the $\hat{\mathbf{z}}$ direction. The magnetic fluctuations are the real part of

$$\tilde{M}_{x,y}(\mathbf{r},t) = \tilde{m}_{x,y}\Theta(x)\Theta(-x+d)\Theta(y+w/2)\Theta(-y+w/2)e^{-i\omega t}, \tag{5}$$

where d and w are the thickness and width of the nanowire. The corresponding dipolar magnetic field

$$\tilde{h}_\beta(\mathbf{r},t) = \frac{1}{4\pi}\partial_\beta\partial_\alpha\int\frac{\tilde{M}_\alpha(\mathbf{r}',t)}{|\mathbf{r}-\mathbf{r}'|}d\mathbf{r}' = \frac{1}{4\pi}\partial_\beta\partial_\alpha\int dz'\int_0^d dx'\int_{-w/2}^{w/2}dy'\frac{\tilde{m}_\alpha e^{-i\omega t}}{\sqrt{z'^2+(x-x')^2+(y-y')^2}}. \tag{6}$$

By substituting the Coulomb integral [1, 2],

$$\frac{1}{\sqrt{z'^2+(x-x')^2+(y-y')^2}} = \frac{1}{2\pi}\int dk_x dk_y\frac{e^{-|z'|\sqrt{k_x^2+k_y^2}}}{\sqrt{k_x^2+k_y^2}}e^{ik_x(x-x')+ik_y(y-y')}, \tag{7}$$

the magnetic field below the nanowire ($x<0$) with Fourier component k_y

$$\begin{aligned}\tilde{h}_\beta(k_y,x,t) &= \int h_\beta(\mathbf{r},t)e^{-ik_y y}dy \\ &= \frac{1}{2\pi}\int dk_x(k_x\tilde{m}_x+k_y\tilde{m}_y)k_\beta e^{ik_x x-i\omega t}\frac{1}{k_x^2+k_y^2}\frac{1}{ik_x}(1-e^{-ik_x d})\frac{2\sin(k_y w/2)}{k_y}.\end{aligned} \tag{8}$$

Closing the contour of the k_x integral in the lower half complex plane

$$\begin{pmatrix}\tilde{h}_x(k_y,x,t) \\ \tilde{h}_y(k_y,x,t)\end{pmatrix} = -\frac{i}{4\pi}e^{|k_y|x}(1-e^{-|k_y|d})\frac{2\sin(k_y w/2)}{k_y|k_y|}\begin{pmatrix}|k_y| & ik_y \\ ik_y & -|k_y|\end{pmatrix}\begin{pmatrix}\tilde{m}_x \\ \tilde{m}_y\end{pmatrix}e^{-i\omega t}. \tag{9}$$

A perfectly right circularly polarized wire dynamics ($\tilde{m}_y = i\tilde{m}_x$) implies that the Fourier components of $\tilde{\mathbf{h}}$ with $k_y>0$ vanish. The Fourier component with $k_y<0$ is perfectly left circularly polarized $\left(\tilde{h}_y = -i\tilde{h}_x\right)$.

II. ANGLE-DEPENDENT DIPOLAR COUPLING

Here we address the dependence of the coupling when the film magnetization rotates in the film while the nanowire magnetization is kept constant. We choose a rotated coordinate system in which the equilibrium magnetizations of nanowire and film are $\tilde{M}_s(0,\sin\theta,\cos\theta)$ and $M_s\hat{\mathbf{z}}$, as shown in Fig. 1. The two components of the dynamic

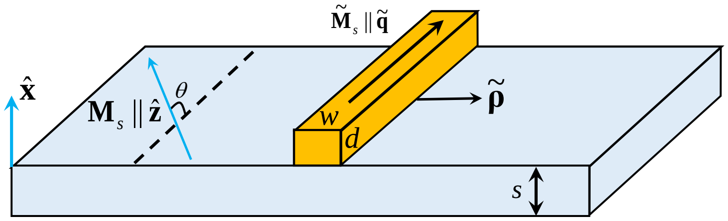

FIG. 1. (Color online) Parameters and coordinate system when the magnetizations of film and nanowire are non-collinear.

magnetization in the nanowire relative to the film magnetization are $\tilde{\mathbf{M}}_{\perp}(\mathbf{r}) \parallel \left(\tilde{\mathbf{M}}_s/\tilde{M}_s \cdot \hat{\mathbf{x}}\right)\hat{\mathbf{x}}$ and $\tilde{\mathbf{M}}_{\parallel}(\mathbf{r}) \parallel \left(\tilde{\mathbf{M}}_s/\tilde{M}_s\right) \times \hat{\mathbf{x}}$. The Zeeman interaction with a magnetic field $\mathbf{h}$ emitted by the film reads

$$\begin{aligned} H_{\rm int} &= -\mu_0 \int_0^d \left\{ \tilde{M}_{\perp}(\mathbf{r}) h_x(\mathbf{r}) + \left[\tilde{M}_{\parallel}(\mathbf{r}) \cos\theta + \tilde{M}_s \sin\theta \right] h_y(\mathbf{r}) + \left[-\tilde{M}_{\parallel}(\mathbf{r}) \sin\theta + \tilde{M}_s \cos\theta \right] h_z(\mathbf{r}) \right\} dx d\boldsymbol{\rho} \\ &\to -\mu_0 \int_0^d \left[\tilde{M}_{\perp}(\mathbf{r}) h_x(\mathbf{r}) + \tilde{M}_{\parallel}(\mathbf{r}) h_y(\mathbf{r}) \cos\theta - \tilde{M}_{\parallel}(\mathbf{r}) h_z(\mathbf{r}) \sin\theta \right] dx d\boldsymbol{\rho}. \end{aligned} \tag{10}$$

The spatial integral is over the nanowire with thickness d and in the second step we disregard the fluctuating torques on the equilibrium magnetization. The magnetization operator $\hat{M}_\alpha$ in the film may be expanded into the magnon field operators $\hat{\alpha}_{\mathbf{k}}$ and $\hat{\alpha}_{\mathbf{k}}^\dagger$ with Boson commutator $[\hat{\alpha}_{\mathbf{k}}, \hat{\alpha}_{\mathbf{k}'}^\dagger] = \delta_{\mathbf{k}\mathbf{k}'}$

$$\hat{M}_\alpha(\mathbf{r}) = -\sqrt{2M_s\gamma\hbar} \sum_{\mathbf{k}} \left(m_\alpha^{\mathbf{k}}(x) e^{i\mathbf{k}\cdot\boldsymbol{\rho}} \hat{\alpha}_{\mathbf{k}} + \overline{m_\alpha^{\mathbf{k}}(x)} e^{-i\mathbf{k}\cdot\boldsymbol{\rho}} \hat{\alpha}_{\mathbf{k}}^\dagger \right), \tag{11}$$

where $\overline{A} = A^*$ and $m_\alpha^{\mathbf{k}}(x)$ is the amplitude of the spin waves over the film thickness. The magnons of nanowire propagate with momentum $\tilde{\mathbf{q}} = \tilde{q}(\sin\theta\hat{\mathbf{y}} + \cos\theta\hat{\mathbf{z}}) = \tilde{q}\mathbf{e}_n$ along the nanowire. In terms of the magnon field operators $\hat{\beta}_{\tilde{\mathbf{q}}}$, $\hat{\beta}_{\tilde{\mathbf{q}}}^\dagger$ with $[\hat{\beta}_{\tilde{\mathbf{q}}}, \hat{\beta}_{\tilde{\mathbf{q}}'}^\dagger] = \delta_{\tilde{\mathbf{q}}\tilde{\mathbf{q}}'}$

$$\hat{\tilde{M}}_\delta(\mathbf{r}) = -\sqrt{2\tilde{M}_s\gamma\hbar} \sum_{\tilde{q}} \left(\tilde{m}_\delta^{\tilde{\mathbf{q}}}(\tilde{\boldsymbol{\rho}}) e^{i\tilde{q}\tilde{z}} \hat{\beta}_{\tilde{\mathbf{q}}} + \overline{\tilde{m}_\delta^{\tilde{\mathbf{q}}}(\tilde{\boldsymbol{\rho}})} e^{-i\tilde{q}\tilde{z}} \hat{\beta}_{\tilde{\mathbf{q}}}^\dagger \right), \tag{12}$$

where $\delta = \{\perp, \parallel\}$, $\tilde{z} = y\sin\theta + z\cos\theta$, and $\tilde{\boldsymbol{\rho}} = x\hat{\mathbf{x}} + \tilde{y}(\cos\theta\hat{\mathbf{y}} - \sin\theta\hat{\mathbf{z}})$ is a vector in the nanowire cross section with $-w/2 \le \tilde{y} \le w/2$ and $0 \le x \le d$.

Using the dipolar field Eq. (1)

$$\hat{h}_\beta(\mathbf{r}) = \frac{1}{4\pi} \partial_\beta \partial_\alpha \int d\mathbf{r}' \frac{\hat{M}_\alpha(\mathbf{r}')}{|\mathbf{r} - \mathbf{r}'|}, \tag{13}$$

and substituting Eqs. (11) and (12) into Eq. (10) yields

$$\hat{H}_{\rm int} = \sum_{\mathbf{k}} \left(g_{\mathbf{k}} \hat{\alpha}_{\mathbf{k}}^\dagger \hat{\beta}_{k_\parallel \mathbf{e}_n} + \text{h.c.} \right), \tag{14}$$

where $k_\parallel = k_y \sin\theta + k_z \cos\theta$, the coupling constant

$$g_{\mathbf{k}} = -2\mu_0\gamma\hbar\sqrt{\tilde{M}_s M_s} \frac{1}{k_\perp} \sin\left(\frac{k_\perp w}{2}\right) \int_0^d dx \int_{-s}^0 dx'^{-(x-x')|\mathbf{k}|} \left(\overline{m_x^{\mathbf{k}}(x')}, \overline{m_y^{\mathbf{k}}(x')} \right) \begin{pmatrix} |\mathbf{k}| & ik_\perp \\ ik_y & -\frac{k_y k_\perp}{|\mathbf{k}|} \end{pmatrix} \begin{pmatrix} \tilde{m}_\perp^{k_\parallel \mathbf{e}_n}(x) \\ \tilde{m}_\parallel^{k_\parallel \mathbf{e}_n}(x) \end{pmatrix},$$

and $k_\perp = -k_z \sin\theta + k_y \cos\theta$. For thin films the magnetization is constant over the film (s) and nanowire (d) thickness and

$$g_{\mathbf{k}} \to -2\mu_0\gamma\hbar\sqrt{\tilde{M}_s M_s}\frac{1}{k_\perp|\mathbf{k}|^2}\sin\left(\frac{k_\perp w}{2}\right)\left(1-e^{-|\mathbf{k}|d}\right)\left(1-e^{-|\mathbf{k}|s}\right)\left(\overline{m_x^{\mathbf{k}}},\overline{m_y^{\mathbf{k}}}\right)\begin{pmatrix}|\mathbf{k}| & ik_\perp\\ ik_y & -\frac{k_y k_\perp}{|\mathbf{k}|}\end{pmatrix}\begin{pmatrix}\tilde{m}_\perp^{k_\parallel \mathbf{e}_n}\\ \tilde{m}_\parallel^{k_\parallel \mathbf{e}_n}\end{pmatrix}.$$

The normalized magnon amplitudes of exchange spin waves in the film [1, 3, 4]

$$m_y^{\mathbf{k}} = i m_x^{\mathbf{k}} = i\sqrt{1/(4s)}, \tag{15}$$

and those in the nanowire are

$$\tilde{m}_\perp^{k_\parallel \mathbf{e}_n} = \sqrt{\frac{1}{4\mathcal{D}(k_\parallel)wd}}, \qquad \tilde{m}_\parallel^{k_\parallel \mathbf{e}_n} = i\sqrt{\frac{\mathcal{D}(k_\parallel)}{4wd}}, \tag{16}$$

where

$$\mathcal{D}(k_\parallel) = \sqrt{\frac{H_{\rm app} + N_{xx}\tilde{M}_s + \tilde{\lambda}_{\rm ex}k_\parallel^2\tilde{M}_s}{H_{\rm app} + N_{yy}\tilde{M}_s + \tilde{\lambda}_{\rm ex}k_\parallel^2\tilde{M}_s}}. \tag{17}$$

$H_{\rm app}$ and $\tilde{\lambda}_{\rm ex}$ are the applied magnetic field and the exchange stiffness of the nanowire, respectively. The demagnetization factors are estimated to be $N_{xx} \simeq w/(d+w)$ and $N_{yy} = d/(d+w)$ [1] also govern the Kittel mode frequency

$$\omega_{\rm K} = \mu_0\gamma\sqrt{(H_{\rm app} + N_{yy}\tilde{M}_s)(H_{\rm app} + N_{xx}\tilde{M}_s)}. \tag{18}$$

We can now discuss special configurations.

(i) When magnetizations are antiparallel, $\theta = \pi$, $k_\parallel = -k_z$, $k_\perp = -k_y$, and $\mathbf{e}_n = -\hat{\mathbf{z}}$. The coupling strength

$$g_{\mathbf{k}}^{\parallel} \to -2\mu_0\gamma\hbar\sqrt{\tilde{M}_s M_s}\frac{1}{k_y|\mathbf{k}|^2}\sin\left(\frac{k_y w}{2}\right)\left(1-e^{-|\mathbf{k}|d}\right)\left(1-e^{-|\mathbf{k}|s}\right)\left(\overline{m_x^{\mathbf{k}}},\overline{m_y^{\mathbf{k}}}\right)\begin{pmatrix}|\mathbf{k}| & -ik_y\\ ik_y & \frac{k_y^2}{|\mathbf{k}|}\end{pmatrix}\begin{pmatrix}\tilde{m}_\perp^{k_z\hat{\mathbf{z}}}\\ \tilde{m}_\parallel^{k_z\hat{\mathbf{z}}}\end{pmatrix}. \tag{19}$$

In the notation of the main text, $\tilde{m}_\perp^{k_z\hat{\mathbf{z}}} = \tilde{m}_x^{(k_z)}$ and $\tilde{m}_\parallel^{k_z\hat{\mathbf{z}}} = -\tilde{m}_y^{(k_z)}$. When both spin waves in the film and nanowire are circularly polarized the chirality is perfect and the coupling strength is maximized.

(ii) When magnetizations are normal to each other, $\theta = \pi/2$, $k_\parallel = k_y$, $k_\perp = -k_z$, $\mathbf{e}_n = \hat{\mathbf{y}}$, and

$$g_{\mathbf{k}}^{\perp} \to -2\mu_0\gamma\hbar\sqrt{\tilde{M}_s M_s}\frac{1}{k_z|\mathbf{k}|^2}\sin\left(\frac{k_z w}{2}\right)\left(1-e^{-|\mathbf{k}|d}\right)\left(1-e^{-|\mathbf{k}|s}\right)\left(\overline{m_x^{\mathbf{k}}},\overline{m_y^{\mathbf{k}}}\right)\begin{pmatrix}|\mathbf{k}| & -ik_z\\ ik_y & \frac{k_y k_z}{|\mathbf{k}|}\end{pmatrix}\begin{pmatrix}\tilde{m}_\perp^{k_y\hat{\mathbf{y}}}\\ \tilde{m}_\parallel^{k_y\hat{\mathbf{y}}}\end{pmatrix}. \tag{20}$$

The coupling to travelling waves in the nanowire with finite k_y is not perfectly chiral, even for the circularly polarized spin waves in the film and nanowire, but still directional, depending on k_y/k_z.

(iii) In the limit of coherent excitation of only the Kittel mode $k_\parallel = 0$, but at arbitrary angle $k_y = k_\perp\cos\theta$,

$$g_{k_\perp}^{\rm K} \to -2\mu_0\gamma\hbar\sqrt{\tilde{M}_s M_s}\frac{1}{k_\perp^3}\sin\left(\frac{k_\perp w}{2}\right)\left(1-e^{-|k_\perp|d}\right)\left(1-e^{-|k_\perp|s}\right)\left(\overline{m_x^{\mathbf{k}}},\overline{m_y^{\mathbf{k}}}\cos\theta\right)\begin{pmatrix}|k_\perp| & ik_\perp\\ ik_\perp & -|k_\perp|\end{pmatrix}\begin{pmatrix}\tilde{m}_\perp^{(0)}\\ \tilde{m}_\parallel^{(0)}\end{pmatrix}. \tag{21}$$

The Kittel mode in the nanowire with right circular polarization couples with the spin waves propagating perpendicular to the nanowire with perfect chirality (Sec. I B). In general, the Kittel mode in the nanowire is elliptic; the chirality can then be tuned by the angle θ. In particular, the ellipticity leads to a "magic" angle θ_c at which the chirality of the (nonzero) coupling vanishes. Using $\left|g^{\rm K}_{k_\perp}\right| = |g^{\rm K}_{-k_\perp}|$ and assuming pure exchange spin waves in the film [Eq. (15)],

$$\cos\theta_c = -i\tilde{m}^{(0)}_{\parallel}/\tilde{m}^{(0)}_{\perp} \;\text{ or }\; i\tilde{m}^{(0)}_{\perp}/\tilde{m}^{(0)}_{\parallel}.$$

In the limit of small applied magnetic fields, Eq. (16) yields $\tilde{m}^{(0)}_{\perp} \simeq \sqrt{1/(4w\sqrt{wd})}$ and $\tilde{m}^{(0)}_{\parallel} \simeq i\sqrt{1/(4d\sqrt{wd})}$. With $w > d$, the critical angle is governed by the aspect ratio with $\cos\theta_c \simeq \sqrt{d/w}$. When $d \to w$ the Kittel mode is circularly polarized and the chirality vanishes with the coupling constant when approaching the parallel configuration.

III. LINEAR RESPONSE THEORY OF CHIRAL MAGNON EXCITATION

The coherent excitation of a magnetization by a proximity magnetic transducer can alternatively be formulated by linear response theory [5, 6]. The excited magnetization in the film can be expressed by time-dependent perturbation theory as:

$$M_\alpha(x,\boldsymbol{\rho},t) = -i\int_{-\infty}^{t} dt' \left\langle \left[\hat{M}_\alpha(x,\boldsymbol{\rho},t), \hat{H}_{\rm int}(t')\right]\right\rangle . \tag{22}$$

In terms of the retarded spin susceptibility

$$\chi_{\alpha\delta}(x,x';\boldsymbol{\rho}-\boldsymbol{\rho}';t-t') = i\Theta(t-t')\left\langle\left[\hat{S}_\alpha(x,\boldsymbol{\rho},t),\hat{S}_\delta(x',\boldsymbol{\rho}',t')\right]\right\rangle, \tag{23}$$

where $\hat{S}_\alpha = -\hat{M}_\alpha/(\gamma\hbar)$ is the spin operator,

$$M_\alpha(x,\boldsymbol{\rho},t) = \mu_0(\gamma\hbar)^2\sum_{\mathbf{k}}\int_{-\infty}^{\infty}dt'\int_0^d d\tilde{x}d\tilde{\boldsymbol{\rho}}\int_{-s}^{0}dx'\tilde{M}_\beta(\tilde{x},\tilde{\boldsymbol{\rho}},t')G_{\beta\xi}(-\mathbf{k},\tilde{x}-x')\chi_{\alpha\xi}\left(x,x';\mathbf{k};t-t'\right)e^{i\mathbf{k}\cdot(\boldsymbol{\rho}-\tilde{\boldsymbol{\rho}})}.$$

Here $\tilde{\mathbf{M}}$ is the magnetization of the magnetic transducer. With $\tilde{x} > x'$, the Green-function tensor reads

$$G(-\mathbf{k},\tilde{x}-x') = \frac{e^{-|\tilde{x}-x'||\mathbf{k}|}}{2}\begin{pmatrix} |\mathbf{k}| & ik_y & ik_z \\ ik_y & -k_y^2/|\mathbf{k}| & -k_yk_z/|\mathbf{k}| \\ ik_z & -k_yk_z/|\mathbf{k}| & -k_z^2/|\mathbf{k}| \end{pmatrix}. \tag{24}$$

In terms of eigenmodes $m^{\mathbf{k}}_\alpha(x)e^{i\mathbf{k}\cdot\boldsymbol{\rho}}$ and their frequency $\omega_{\mathbf{k}}$,

$$\chi_{\alpha\xi}(x,x';\mathbf{k};\omega) = -\frac{2M_s}{\gamma\hbar}m^{\mathbf{k}}_\alpha(x)\overline{m^{\mathbf{k}}_\xi(x)}\frac{1}{\omega-\omega_{\mathbf{k}}+i0_+} \tag{25}$$

is the spin susceptibility in momentum-frequency space. The excited magnetization is

$$\begin{aligned} M_\alpha(x,\boldsymbol{\rho},t) = {}& -2\mu_0 M_s\gamma\hbar\sum_{\mathbf{k}}\int_{-\infty}^{\infty}dt'\int_0^d d\tilde{x}d\tilde{\boldsymbol{\rho}}\int_{-s}^{0}dx'\int\frac{d\omega}{2\pi}e^{-i\omega(t-t')+i\mathbf{k}\cdot(\boldsymbol{\rho}-\tilde{\boldsymbol{\rho}})}\frac{1}{\omega-\omega_{\mathbf{k}}+i0_+} \\ & \times m^{\mathbf{k}}_\alpha(x)\tilde{M}_\beta(\tilde{x},\tilde{\boldsymbol{\rho}},t')G_{\beta\xi}(-\mathbf{k},\tilde{x}-x')\overline{m^{\mathbf{k}}_\xi(x)}. \end{aligned} \tag{26}$$

Under steady-state resonant microwave excitation of the Kittel mode Eq. (A18)

$$\tilde{M}_\beta(\tilde{x},\tilde{\boldsymbol{\rho}},t') \approx \tilde{M}_\beta(\tilde{x},\tilde{\boldsymbol{\rho}},t)e^{i\omega_{\rm K}(t-t')}, \tag{27}$$

the film magnetization becomes

$$M_\alpha(x,\boldsymbol{\rho},t) = -2\mu_0 M_s\gamma\hbar\sum_{\mathbf{k}}\int_0^d d\tilde{x}d\tilde{\boldsymbol{\rho}}\int_{-s}^0 dx' e^{i\mathbf{k}\cdot(\boldsymbol{\rho}-\tilde{\boldsymbol{\rho}})}\frac{1}{\omega_{\mathrm{K}}-\omega_{\mathbf{k}}+i0_+}m_\alpha^{\mathbf{k}}(x)\tilde{M}_\beta(\tilde{x},\tilde{\boldsymbol{\rho}},t)G_{\beta\xi}(-\mathbf{k},\tilde{x}-x')\overline{m_\xi^{\mathbf{k}}(x)}.$$

When nanowire and equilibrium magnetizations are parallel to $\hat{\mathbf{z}}$, the momentum integral in

$$\begin{aligned} M_\alpha(x,y,t) = -2\mu_0 M_s\gamma\hbar\int\frac{dk_y}{2\pi}\int_0^d d\tilde{x}d\tilde{y}\int_{-s}^0 dx' e^{ik_y(y-\tilde{y})}\frac{1}{\omega_{\mathrm{K}}-\omega_{k_y}+i0_+} \\ \times\, m_\alpha^{k_y}(x)M_\beta(\tilde{x},\tilde{y},t)G_{\beta\xi}(-k_y,\tilde{x}-x')\overline{m_\xi^{k_y}(x)} \end{aligned} \tag{28}$$

can be evaluated by contours in the complex plane. The zeros of the denominator $\omega_{\mathrm{K}}-\omega_{k_y}+i0_+$ generate two singularities at $k_\pm=\pm(k_*+i0_+)$ with $k_*>0$, so k_+ and k_- lie in the upper and lower half planes, respectively. When $y>\tilde{y}$ the contour should be closed in the upper half plane and

$$M_\alpha^>(x,y,t) = 2i\mu_0 M_s\gamma\hbar\frac{1}{v_{k_*}}\int_0^d d\tilde{x}d\tilde{y}\int_{-s}^0 dx' e^{ik_*(y-\tilde{y})}m_\alpha^{k_*}(x)M_\beta(\tilde{x},\tilde{y},t)G_{\beta\xi}(-k_*,\tilde{x}-x')\overline{m_\xi^{k_*}(x)}, \tag{29}$$

where $v_{k_*}=\partial\omega_k/\partial k|_{k=k_*}$ is the spin wave group velocity. A small or zero group velocity implies a large density of states and excitation efficiency. When $y<\tilde{y}$,

$$M_\alpha^<(x,y,t) = 2i\mu_0 M_s\gamma\hbar\frac{1}{v_{k_*}}\int_0^d d\tilde{x}d\tilde{y}\int_{-s}^0 dx' e^{-ik_*(y-\tilde{y})}m_\alpha^{-k_*}(x)M_\beta(\tilde{x},\tilde{y},t)G_{\beta\xi}(k_*,\tilde{x}-x')\overline{m_\xi^{-k_*}(x)}. \tag{30}$$

When the spin waves in the film are circularly polarized with $m_y=im_x$,

$$G_{\beta\xi}(-k_*,\tilde{x}-x')\overline{m_\xi^{k_*}(x)} \longrightarrow \frac{e^{-|\tilde{x}-x'||k_*|}}{2}\begin{pmatrix} k_* & ik_* \\ ik_* & -k_*\end{pmatrix}\begin{pmatrix} m_x \\ -im_x\end{pmatrix} = \begin{pmatrix} 0 \\ 0\end{pmatrix}, \tag{31}$$

leading to zero $M_\alpha^<(x,y,t)$, but finite $M_\alpha^>(x,y,t)$. So the nanowire can only excite spin waves with positive momentum. Also, energy and momentum is injected into only half of the film with $y>\tilde{y}$. This "spatial chirality" persists in the limit of vanishing dissipation and is a consequence of the causality or retardation.

IV. SCATTERING MATRIX OF MICROWAVE PHOTONS

The magnetic order in two nanowires located at $\mathbf{r}_1=R_1\hat{\mathbf{y}}$ and $\mathbf{r}_2=R_2\hat{\mathbf{y}}$ may act as transducers for microwaves that are emitted or detected by local microwave antennas as well as excite and detect magnons in the film. We are interested in the observable—the scattering matrix of the microwaves with excitation (input) at R_1 and the detection (output) at R_2, which can be formulated by the input-output theory [7, 8]. When the local magnon states at R_1 and R_2 are expressed by the operators $\hat{m}_L$ and $\hat{m}_R$, respectively, this leads to the equations of motion of the coupled nanowires and the film

$$\begin{aligned} \frac{d\hat{m}_L}{dt} &= -i\omega_{\mathrm{K}}\hat{m}_L(t) - i\sum_q g_q e^{iqR_1}\hat{\alpha}_q(t) - \left(\frac{\kappa_L}{2}+\frac{\kappa_{p,L}}{2}\right)\hat{m}_L(t) - \sqrt{\kappa_{p,L}}\hat{p}_{\mathrm{in}}^{(L)}(t), \\ \frac{d\hat{m}_R}{dt} &= -i\omega_{\mathrm{K}}\hat{m}_R(t) - i\sum_q g_q e^{iqR_2}\hat{\alpha}_q(t) - \frac{\kappa_R}{2}\hat{m}_R(t), \\ \frac{d\hat{\alpha}_q}{dt} &= -i\omega_q\hat{\alpha}_q(t) - ig_q e^{-iqR_1}\hat{m}_L(t) - ig_q e^{-iqR_2}\hat{m}_R(t) - \frac{\kappa_q}{2}\hat{\alpha}_q(t). \end{aligned} \tag{32}$$

Here, κ_L and κ_R are the intrinsic damping of the Kittel modes in the left and right nanowires, respectively, $\kappa_{p,L}$ is the additional radiative damping induced by the microwave photons $\hat{p}_{\text{in}}^{(L)}$, i.e. the coupling of the left nanowire with the microwave source, and κ_q denotes the intrinsic (Gilbert) damping of magnons in the films. In frequency space:

$$\begin{aligned}
\hat{\alpha}_q(\omega) &= g_q G_q(\omega)\left[e^{-iqR_1}\hat{m}_L(\omega) + e^{-iqR_2}\hat{m}_R(\omega)\right], \\
\hat{m}_R(\omega) &= \frac{-i\sum_q g_q^2 G_q(\omega)\, e^{iq(R_2-R_1)}}{-i(\omega-\omega_{\text{K}}) + \kappa_R/2 + i\sum_q g_q^2 G_q(\omega)}\hat{m}_L(\omega), \\
\hat{m}_L(\omega) &= \frac{-\sqrt{\kappa_{p,L}}}{-i(\omega-\omega_{\text{K}}) + (\kappa_L+\kappa_{p,L})/2 + i\sum_q g_q^2 G_q(\omega) - f(\omega)}\hat{p}_{\text{in}}^{(L)}(\omega),
\end{aligned} \tag{33}$$

where $G_q(\omega) = [(\omega-\omega_q) + i\kappa_q/2]^{-1}$ and

$$f(\omega) \equiv -\frac{\left(\sum_q g_q^2 G_q(\omega)\, e^{iq(R_1-R_2)}\right)\left(\sum_q g_q^2 G_q(\omega)\, e^{iq(R_2-R_1)}\right)}{-i(\omega-\omega_{\text{K}}) + \kappa_R/2 + i\sum_q g_q^2 G_q(\omega)}. \tag{34}$$

For perfect chiral coupling $f(\omega)$ vanishes by the absence of back-action. The excitation of the left nanowire propagates to the right nanowire by the spin waves in the film. The microwave output of the left and right nanowires inductively detected by coplanar wave guides are denoted by $\hat{p}_{\text{out}}^{(L)}(\omega)$ and $\hat{p}_{\text{out}}^{(R)}(\omega)$ with input-output relations [7, 8]

$$\begin{aligned}
\hat{p}_{\text{out}}^{(L)}(\omega) &= p_{\text{in}}^{(L)}(\omega) + \sqrt{\kappa_{p,L}}\hat{m}_L(\omega), \\
\hat{p}_{\text{out}}^{(R)}(\omega) &= \sqrt{\kappa_{p,R}}\hat{m}_R(\omega),
\end{aligned} \tag{35}$$

where $\kappa_{p,R}$ is the additional radiative damping induced by the detector. Therefore, the elements in the microwave scattering matrix, i.e., microwave reflection (S_{11}) and transmission (S_{21}) amplitudes become

$$\begin{aligned}
S_{11}(\omega) &\equiv \frac{\hat{p}_{\text{out}}^{(L)}}{\hat{p}_{\text{in}}^{(L)}} = 1 - \frac{\kappa_{p,L}}{-i(\omega-\omega_{\text{K}}) + (\kappa_L+\kappa_{p,L})/2 + i\sum_q g_q^2 G_q(\omega) - f(\omega)}, \\
S_{21}(\omega) &\equiv \frac{\hat{p}_{\text{out}}^{(R)}}{\hat{p}_{\text{in}}^{(L)}} = [1 - S_{11}(\omega)]\sqrt{\frac{\kappa_{p,R}}{\kappa_{p,L}}}\frac{i\sum_q g_q^2 G_q(\omega)\, e^{iq(R_2-R_1)}}{-i(\omega-\omega_{\text{K}}) + \kappa_R/2 + i\sum_q g_q^2 G_q(\omega)}.
\end{aligned} \tag{36}$$

The real parts of S_{11} and S_{12} are illustrated in Fig. 2 when the magnetizations of nanowire and film are antiparallel. the interference patterns on the Kittel resonance of cobalt nanowire in Fig. 2(b) reflect the interaction between nanowires and film. The phase factor $e^{ik(R_1-R_2)}$ in Eq. (36) provides peaks and dips when the resonant momentum k is modulated. These patterns are not caused by spin wave interference in the film since in our model the nanowires cannot reflect spin waves.

V. DIPOLAR NON-LOCAL SPIN SEEBECK EFFECT

We consider two identical transducers, with a magnetic nanowire at $\mathbf{r}_2 = R_2\hat{\mathbf{y}}$ that detects thermally injected magnons by a nanowire at $\mathbf{r}_1 = R_1\hat{\mathbf{y}}$ with $R_1 < R_2$ mediated by the dipolar interaction only. For simplicity, we consider only the Kittel modes in the wires, which is a good approximation at low temperatures at which higher modes are frozen out. The contribution by higher modes with large wave numbers k is disregarded because the

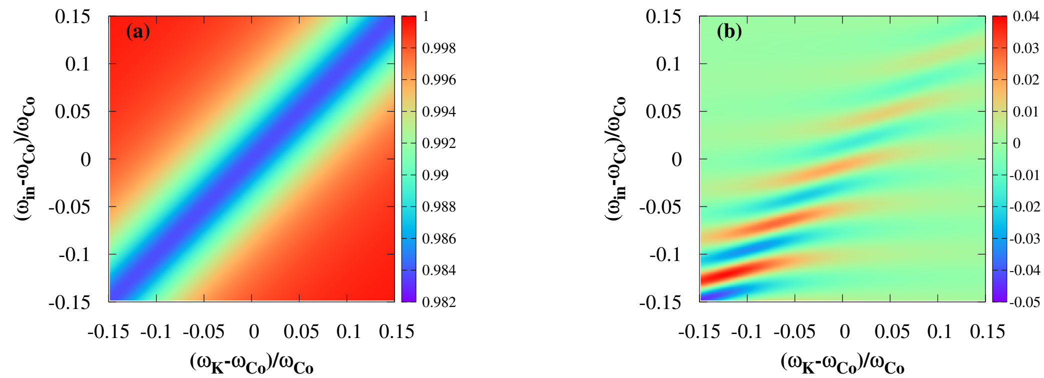

FIG. 2. (Color online) Reflection $\mathrm{Re}(S_{11})$ [(a)] and transmission $\mathrm{Re}(S_{12})$ [(b)] amplitudes of microwaves, Eq. (A36) between two magnetic nanowires on a magnetic film. ω_{Co} is the Kittel mode frequency Eq. (18) of the cobalt nanowire at a small applied field ($H_{\mathrm{app}} = 0.05$ T) that fixes an antiparallel magnetizations, ω_{in} is the frequency of the input microwaves, and ω_{K} is the Kittel mode frequency as a function of an applied field H_{app}. The radiative coupling of both nanowires $\kappa_p/(2\pi) = 10$ MHz while other parameter values are listed in the main text.

dipolar coupling is exponentially suppressed $\sim e^{-kx}$. The coupling strength $|g_{\mathbf{k}}|$ in Fig. 3 illustrates that magnons with wavelength around half of the nanowire width ($\pi/w = 0.045$ nm^{-1}) dominate the coupling. Thermal pumping from other than the Kittel mode can be disregarded even at elevated temperatures. Furthermore, the spin current in the film is dominated by spin waves with small momentum and long mean-free paths, so in the following we may disregard the effects of magnon-magnon and magnon-phonon interactions that otherwise render magnon transport phenomena diffuse [9]. The narrow-band thermal injection also favors the inductive detection of the injected spin current pursued here, rather than by the inverse spin Hall effect with heavy metal contacts.

The equation of motions of the Kittel modes in the nanowire and film spin waves in the coupled system read

$$\begin{aligned}
\frac{d\hat{m}_L}{dt} &= -i\omega_{\mathrm{K}}\hat{m}_L - \sum_q ig_q^* e^{iqR_1}\hat{\alpha}_q - \frac{\kappa}{2}\hat{m}_L - \sqrt{\kappa}\hat{N}_L,\\
\frac{d\hat{m}_R}{dt} &= -i\omega_{\mathrm{K}}\hat{m}_R - \sum_q ig_q^* e^{iqR_2}\hat{\alpha}_q - \frac{\kappa}{2}\hat{m}_R - \sqrt{\kappa}\hat{N}_R,\\
\frac{d\hat{\alpha}_q}{dt} &= -i\omega_q\hat{\alpha}_q - ig_q e^{-iqR_1}\hat{m}_L - ig_q e^{-iqR_2}\hat{m}_R - \frac{\kappa_q}{2}\hat{\alpha}_q - \sqrt{\kappa_q}\hat{N}_q,
\end{aligned} \tag{37}$$

where κ is caused by the same Gilbert damping in both nanowires, and $\hat{N}_L$ and $\hat{N}_R$ represent the thermal noise in the left and right nanowires, with $\langle \hat{N}_\eta^\dagger(t)\hat{N}_{\eta'}(t')\rangle = n_\eta\delta(t-t')\delta_{\eta\eta'}$. Here, $\eta \in \{L, R\}$ and $n_\eta = 1/\left\{\exp\left[\hbar\omega_{\mathrm{K}}/(k_BT_\eta)\right] - 1\right\}$ and T_R is also the film temperature. Integrating out the spin-wave modes in the film, we obtain equations for dissipatively coupled nanowires. In frequency space,

$$\begin{aligned}
\left(-i(\omega-\omega_{\mathrm{K}}) + \frac{\kappa}{2} + \frac{\Gamma_1+\Gamma_2}{2}\right)\hat{m}_L(\omega) + \Gamma_2 e^{iq_*|R_2-R_1|}\hat{m}_R(\omega) &= \sum_q ig_q^* e^{iqR_1}\sqrt{\kappa_q}G_q(\omega)\hat{N}_q(\omega) - \sqrt{\kappa}\hat{N}_L(\omega),\\
\left(-i(\omega-\omega_{\mathrm{K}}) + \frac{\kappa}{2} + \frac{\Gamma_1+\Gamma_2}{2}\right)\hat{m}_R(\omega) + \Gamma_1 e^{iq_*|R_2-R_1|}\hat{m}_L(\omega) &= \sum_q ig_q^* e^{iqR_2}\sqrt{\kappa_q}G_q(\omega)\hat{N}_q(\omega) - \sqrt{\kappa}\hat{N}_R(\omega),
\end{aligned} \tag{38}$$

where $\Gamma_1 = |g_{q_*}|^2/v_{q_*}$ and $\Gamma_2 = |g_{-q_*}|^2/v_{q_*}$ are assumed constant (for the Kittel mode). Here, q_* is the positive root of $\omega_{q_*} = \omega_{\mathrm{K}}$ as introduced in the main text.

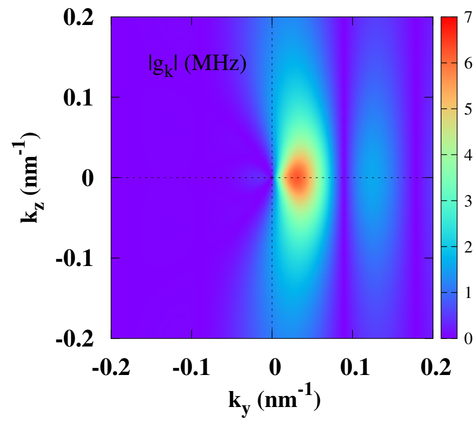

FIG. 3. (Color online) Momentum dependence of the dipolar coupling strength $|g_{\mathbf{k}}|$ between a nanowire and magnetic film for the dimensions and material parameters used in the main text.

For perfectly chiral coupling with $\Gamma_2 = 0$ the solutions of Eqs. (38) read

$$\begin{aligned}\hat{m}_L(\omega) &= \frac{\sum_q i g_q^* e^{iqR_1}\sqrt{\kappa_q}G_q(\omega)\hat{N}_q(\omega) - \sqrt{\kappa}\hat{N}_L(\omega)}{-i(\omega-\omega_{\mathrm{K}}) + \frac{\kappa}{2} + \frac{\Gamma_1}{2}},\\ \hat{m}_R(\omega) &= \frac{\sum_q i g_q^* e^{iqR_2}\sqrt{\kappa_q}G_q(\omega)\hat{N}_q(\omega) - \sqrt{\kappa}\hat{N}_R(\omega) - \Gamma_1 e^{q_*(R_2-R_1)}\hat{m}_L(\omega)}{-i(\omega-\omega_{\mathrm{K}}) + \frac{\kappa}{2} + \frac{\Gamma_1}{2}}.\end{aligned} \tag{39}$$

With $\hat{m}_{L,R}(t) = \int e^{-i\omega t}\hat{m}_{L,R}(\omega)d\omega/(2\pi)$, the non-equilibrium occupation of the Kittel modes becomes

$$\rho_L \equiv \langle \hat{m}_L^\dagger(t)\hat{m}_L(t)\rangle = n_L + \int \frac{d\omega}{2\pi}\frac{\kappa}{(\omega-\omega_{\mathrm{K}})^2 + (\kappa/2+\Gamma_1/2)^2}(n_{q_*} - n_L), \tag{40}$$

$$\rho_R \equiv \langle \hat{m}_R^\dagger(t)\hat{m}_R(t)\rangle = n_R + \int \frac{d\omega}{2\pi}\frac{\Gamma_1^2\kappa}{\left[(\omega-\omega_{\mathrm{K}})^2 + (\kappa/2+\Gamma_1/2)^2\right]^2}(n_L - n_{q_*}), \tag{41}$$

where the damping in the film has been disregarded ($\kappa_q \to 0$). In the linear regime the non-local thermal injection of magnons into the right transducer by the left one then reads

$$\begin{aligned}\delta\rho_R &= \begin{cases} \mathcal{S}_{\mathrm{CSSE}}(T_L - T_R) & \text{when } T_L > T_R \\ 0 & \phantom{\text{when }} T_L \le T_R \end{cases},\\ \mathcal{S}_{\mathrm{CSSE}} &= \int \frac{d\omega}{2\pi}\frac{\Gamma_1^2\kappa}{\left[(\omega-\omega_{\mathrm{K}})^2 + (\kappa/2+\Gamma_1/2)^2\right]^2}\left.\frac{dn_L}{dT}\right|_{T=(T_L+T_R)/2}.\end{aligned} \tag{42}$$

where we defined the chiral (or dipolar) spin Seebeck coefficient $\mathcal{S}_{\mathrm{CSSE}}$.

The magnon diode effect acts a "Maxwell demon" that rectifies fluctuations in the wire temperature. Of course, in thermal equilibrium all right and left moving magnons are eventually connected by reflection of spin waves at the edges and absorption and re-emission by connected heat baths. The Second Law of thermodynamics is therefore safe, but it might be interesting to search for chirality-induced transient effects.

[1] T. Yu, C. P. Liu, H. M. Yu, Y. M. Blanter, and G. E. W. Bauer, Phys. Rev. B **99**, 134424 (2019).

[2] L. Novotny and B. Hecht, *Principles of Nano-Optics* (Cambridge University Press, Cambridge, England, 2006).

[3] L. R. Walker, Phys. Rev. **105**, 390 (1957).

[4] T. Yu, S. Sharma, Y. M. Blanter, and G. E. W. Bauer, Phys. Rev. B **99**, 174402 (2019).

[5] G. D. Mahan, *Many Particle Physics* (Plenum, New York, 1990).

[6] E. Šimánek and B. Heinrich, Phys. Rev. B **67**, 144418 (2003).

[7] C. W. Gardiner and M. J. Collett, Phys. Rev. A **31**, 3761 (1985).

[8] A. A. Clerk, M. H. Devoret, S. M. Girvin, F. Marquardt, and R. J. Schoelkopf, Rev. Mod. Phys. **82**, 1155 (2010).

[9] L. J. Cornelissen, J. Liu, R. A. Duine, J. Ben Youssef, and B. J. van Wees, Nat. Phys. **11**, 1022 (2015).